A General Procedure for the Design of Bulk Acoustic Wave Filters

Lise Catherinot, Sylvain Giraud, Matthieu Chatras, Stéphane Bila, Dominique Cros, T. Baron, S. Ballandras, L. Estagerie, P. Monfraix

A General Procedure for the Design of Bulk Acoustic Wave Filters

Lise Catherinot,[1] Sylvain Giraud,[1] Matthieu Chatras,[1] Stéphane Bila,[1] Dominique Cros,[1] Thomas Baron,[2] Sylvain Ballandras,[2] Laetitia Estagerie,[3] Philippe Monfraix[4]

[1] XLIM, UMR 6172, Université de Limoges/CNRS, 123 Av. Albert Thomas, 87060 Limoges, France
[2] FEMTO-ST, UMR 6174, 32 Rue de l'Observatoire, 25044 Besançon, France
[3] CNES, 18 Av. Edouard Belin, 31401 Toulouse, France
[4] Thalès Alénia Space, 26 Av. Jean-François Champollion, 31100 Toulouse, France

ABSTRACT: This article presents a procedure for the design of bulk acoustic wave (BAW) filters. The procedure consists of optimizing the modified Butterworth-Van Dyke model of each resonator, considering appropriate technological parameters. The approach is demon-strated first to design a classical aluminum nitride-based BAW filter but remains valid for other piezoelectric layers, considering either longitudinal or transverse acoustic wave coupling. The approach is finally applied to the design of a lithium niobate ($LiNbO_3$) BAW filter for wide-band filtering applications.

Keywords: bulk acoustic wave (BAW); microwave filter; filter synthesis; $LiNbO_3$

I. INTRODUCTION

Nowadays, bulk acoustic wave (BAW) devices are used in modern communication systems that require both high integration and performance. BAW devices based, for instance, on aluminum nitride (AlN) or zinc oxide (ZnO) have been extensively studied, and this technology is now an effective alternative for the integration of narrow-band components (5%) such as local oscillators and filters up to some GHz [1–4]. To extend the application of BAW technologies, other piezoelectric materials are investigated and appear as promising solutions for realizing wide-band components.

This article proposes a procedure that can be applied to the design of both narrow-band and wide-band bandpass filters. The design procedure is based on the optimization of a lumped element model of the BAW resonators, which is directly related to the technological parameters.

The context, i.e., the validity, of the proposed approach is discussed, and two examples are chosen for illustration. The first example is a narrow-band (3%) bandpass filter designed for UMTS communications [5]. The second example is a wide-band (25%) bandpass filter designed for space applications.

II. BAW RESONATORS

A. Electromechanical Coupling

Applying an electric field to a piezoelectric crystal produces a mechanical deformation. Moreover, if the crystal is excited with a variable signal, acoustic waves can be generated and propagated. The coupling between electrical and mechanical phenomena is expressed by Eqs. (1-a) and (1-b):

$$T_{ij} = c_{ijkl}S_{kl} - e_{kij}E_k \tag{1a}$$

$$D_j = e_{jkl}S_{kl} + \varepsilon_{jk}E_k, \tag{1b}$$

where T is the mechanical stress (Pa), E is the electric field (V/m), S is the mechanical strain, D is the electric displacement (C/m^2), c is the compliance tensor (Pa), ε is the permittivity tensor (F/m), and e is the piezoelectric tensor (C/m^2).

Solving the previous system of coupled equations, three plane acoustic waves with orthogonal polarizations can propagate, as shown in Figure 1. The quasi-longitudinal wave propagates in the electric field direction, and two quasi-transversal or shear waves propagate in the orthogonal plane, all waves at different velocities.

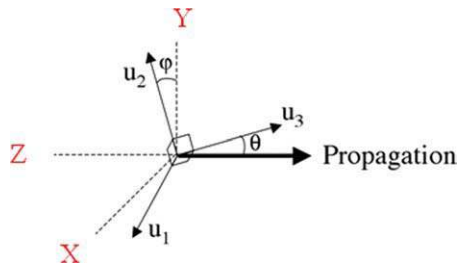

Figure 1 Polarizations of acoustic waves in an anisotropic crystal. [Color figure can be viewed in the online issue, which is available at wileyonlinelibrary.com.]

The conversion of electric energy into mechanical energy is expressed by an electromechanical coupling coefficient, which is related to the physical properties of the material and that is different for the quasi-longitudinal (thickness) wave (k_t^2 or k_{33}^2) and the shear waves (k_s^2 or k_{15}^2). Moreover, because of the anisotropy of piezoelectric materials, electromechanical coupling coefficients also depend on the crystal orientation. Such coefficients can be determined for a given crystal orientation, considering the propagation of a standard plane wave [6]. Assuming a planar geometry of the single-crystal homogeneous plate, one can derive the electromechanical coupling of the wave as a ratio between provided and stored electrical and acoustical energies.

As a result, Figures 2 and 3 present the electromechanical couplings (k_t^2 and k_s^2) of AlN and lithium niobate ($LiNbO_3$), respectively, as a function of the angle (θ) between the propagation direction and the crystallographic orientation. As one can see in Figure 2, the coupling coefficient k_t^2 (thickness wave) is ~7%, whereas k_s^2 is null for a perfectly oriented AlN crystal ($\theta = 180°$). For other orientations, the maximum value of k_s^2 corresponds to a situation where the thickness wave is also coupled ($k_t^2 \neq 0$), and, anyway, the two coupling coefficients are less than 7%. Consequently, AlN is generally used in thickness-mode configuration, and because the bandwidth of the resonator, i.e., of the filter, is directly related to the coupling coefficient, these resonators are restricted to narrow-band applications (<5%).

Observing Figure 3, one can see two interesting orientations for lithium niobate. For $\theta = 126°$ ($Y + 36°$), coefficient k_t^2 is maximum, in the range of 37.5%, and coefficient k_s^2 is approximately null. Inversely, for $\theta = 253°$ ($Y + 163°$), coefficient k_s^2 is in the range of 65.5% when coefficient k_t^2 is null. These two orientations, which are generally used for surface acoustic waves, can be selected for realizing BAW resonators with high electromechanical couplings [7, 8] using either thickness or shear waves.

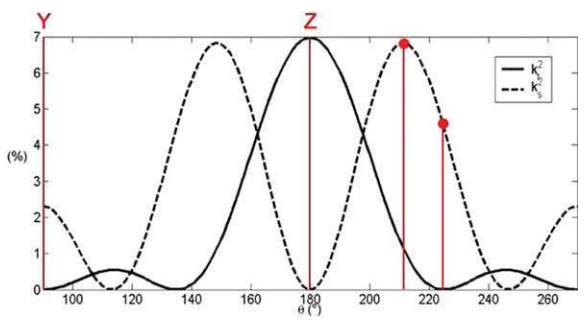

Figure 2 Electromechanical coupling coefficients of AlN. [Color figure can be viewed in the online issue, which is available at wileyonlinelibrary.com.]

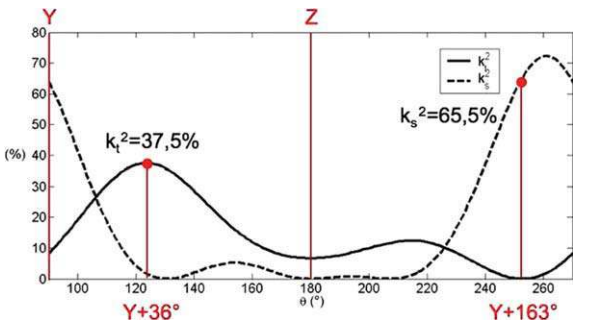

Figure 3 Electromechanical coupling coefficients of $LiNbO_3$. [Color figure can be viewed in the online issue, which is available at wileyonlinelibrary.com.]

Choosing a configuration where only one kind of acoustic wave is excited while the other remains isolated allows to minimize parasitic couplings and to reduce the electromechanical problem to a single dimension. Consequently, with such a configuration, the BAW resonator can be modeled considering a one-dimensional (analytical) model [9] or a classical equivalent circuit (e.g., Mason or Butterworth-Van Dyke) [10].

B. Resonator Structures

BAW resonators are mainly implemented as film (membrane) bulk acoustic resonators (FBARs) or solidly mounted resonators (SMRs). As shown in Figure 4, the acoustic resonance is confined in the piezoelectric layer

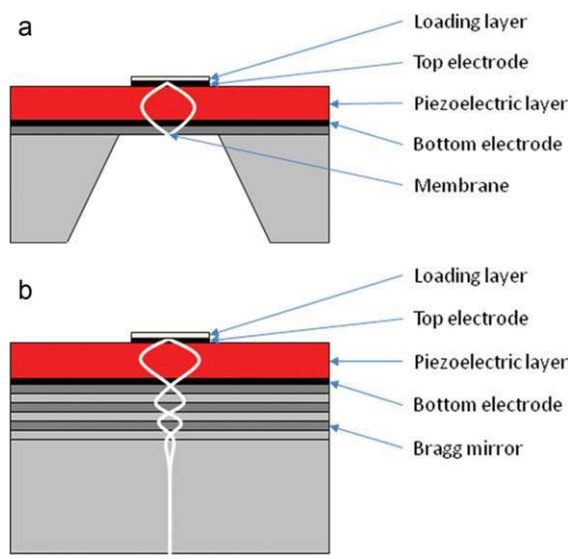

Figure 4 FBAR (a) and SMR (b) structures. [Color figure can be viewed in the online issue, which is available at wileyonlinelibrary.com.]

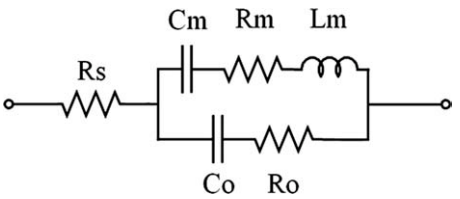

Figure 5 MBVD model of a BAW resonator.

thanks to a membrane for the FBAR structure or thanks to a Bragg mirror for the SMR structure.

The BAW resonator behavior is mainly governed by the thickness of the piezoelectric layer (d) and the surface of the top electrode (A). A loading layer can be deposited on the surface of the top electrode for decreasing the resonant frequencies as explained later in this article.

One can also think about stacked crystal filters or coupled resonator filters [11, 12] as BAW devices, but these structures are not considered in this work.

C. Resonator Model

Under the assumption of a single excited acoustic wave (thickness or shear wave), the BAW resonator can be modeled with the classical MBVD (Modified Butterworth-Van Dyke) circuit given in Figure 5.

This lumped element model represents the electrical impedance of the BAW resonator and can be easily simulated with a circuit software or computed analytically. In the first branch, L_m and C_m represent the acoustic (motional) behavior of the resonator and R_m the mechanical losses. In the second branch, C_o is the electrostatic capacitor and R_o the electrostatic resistance. R_s is a series resistance, which models the electrical losses due to the electrodes.

This equivalent circuit resonates for two particular frequencies:

$$f_s = \frac{1}{2\pi\sqrt{Lm.Cm}} \tag{2a}$$

$$f_p = f_s\sqrt{1+\frac{Cm}{Co}}, \tag{2b}$$

where f_s and f_p are known as the series and parallel resonant frequencies and correspond, respectively, to a minimum and maximum of the electrical impedance as shown in Figure 6. f_s and f_p are related to the electromechanical coupling coefficient $k^2_{t,s}$ by:

$$k^2_{t,s} = \frac{\pi^2}{4}\frac{f_p - f_s}{f_p}. \tag{3}$$

Moreover, one can define Q_s and Q_p, the quality factors of series and parallel resonances:

$$Q_s = \frac{2\pi f_s Lm}{Rm} \tag{4a}$$

$$Q_p = \frac{1}{2\pi f_p CoRo}. \tag{4b}$$

III. FILTER DESIGN

A. Filter Architectures

Ladder and lattice networks are practical architectures, which are widely used for designing BAW resonator filters in FBAR and SMR technologies. As depicted in Figures 7 and 8, these networks combine series and shunt (parallel) resonators to form a bandpass filter device.

For attaining the required filtering function, both the frequencies and the impedances of series and shunt resonators have to be tuned. Because the resonators are fabricated on the same wafer, the thickness of the piezoelectric layer (d) is fixed. Loading the top electrodes is a practical process for altering the resonant frequency of shunt resonators and producing by this way the passband when the admittance of series resonators is high and the admittance of shunt resonators is low.

For adjusting inband and outband characteristics (ripple, return loss, selectivity …), the impedances of individual series (unloaded) and shunt (loaded) resonators have to be tuned. For each resonator, the impedance magnitude is mainly governed by capacitance C_o, which is controlled in practice by the surface of the top electrode (A).

In general, one can observe that ladder networks provide a high selectivity but are limited in terms of out-of-band rejection and that inverse behaviors occur with lattice networks. For achieving both high selectivity and high out-of-band rejection, ladder and lattice networks can be mixed [13] for designing BAW resonator filters.

B. Design Procedure

The synthesis of microwave filters based on coupled electromagnetic (EM) resonators generally starts with the selection of a transfer function (polynomial expression), which satisfies the electrical specifications. In this case, the class of realizable transfer functions is well delimited, and the characteristics of each resonator and coupling

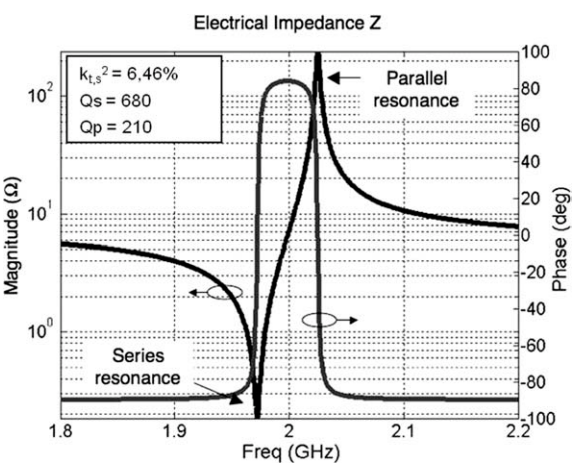

Figure 6 Electrical impedance of a BAW resonator.

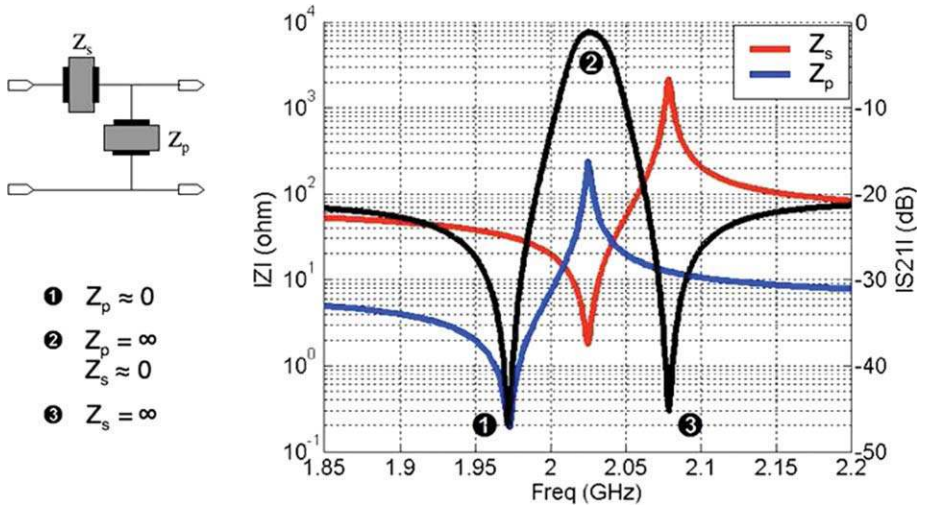

Figure 7 Electrical impedance of shunt and series resonators for providing a bandpass filter with a ladder network. [Color figure can be viewed in the online issue, which is available at wileyonlinelibrary.com.]

element can be derived in a relatively straightforward manner.

Implementing such a methodology for BAW resonator filters is somehow impractical because the class of realizable transfer functions is constrained by the coexistence of close series and parallel resonance frequencies. Furthermore, the BAW technology itself limits the flexibility of filter characteristics, fixing, for example, the same resonance frequencies for each kind of resonator (loaded and unloaded resonators). Consequently, both the intrinsic behavior of BAW resonators and the technology restrict the degrees of freedom for synthesizing a filter, leaving a direct synthesis from the transfer function almost impossible.

On the other hand, the total number of parameters for tuning filter characteristics is limited by the same technological reasons, and this enforces the choice of a local optimization method for synthesizing BAW resonator filters.

Regarding the synthesis, each resonator is characterized by several fixed technological parameters obtained by electromechanical modeling or process characterization: $k^2_{t,s}$, the electromechanical coupling coefficient; Q_s, the quality factor at series resonant frequency; Q_p, the quality factor at parallel resonant frequency; ε_r, the piezoelectric material permittivity; and $R_{[]}$, the square resistance of electrodes.

The remaining variable parameters are as follows: A, the surface of the top electrode ($A = L.W$, where L and W are the length and the width of the top electrode, respectively, but the aspect ratio L/W remains the same for all electrodes). d and l, the thickness of the piezoelectric

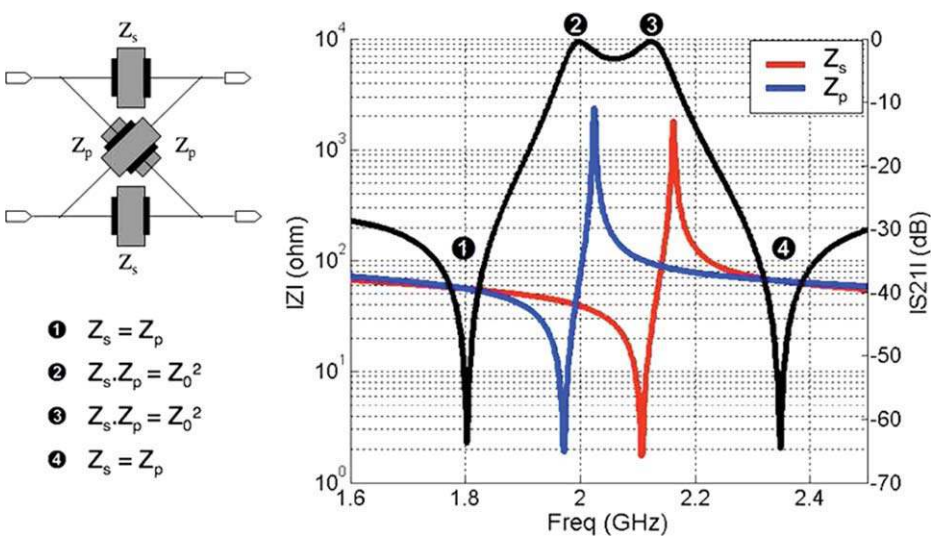

Figure 8 Electrical impedance of shunt and series resonators for providing a bandpass filter with a lattice network. [Color figure can be viewed in the online issue, which is available at wileyonlinelibrary.com.]

layer and the thickness of the loading layer, respectively, which control the series resonant frequencies (f_s) of series and parallel resonators.

The lumped elements of the MBVD model are related to these parameters through the following expressions:

$$C_o = \varepsilon_0 \varepsilon_r \frac{A}{d} \tag{5a}$$

$$C_m = C_o \left[\left(\frac{f_s}{f_p} \right)^2 - 1 \right] \tag{5b}$$

With

$$f_p = \frac{f_s}{1 - \frac{4}{\pi^2} k_{t,s}^2}$$

$$L_m = \frac{1}{C_m (2\pi f_s)^2} \tag{5c}$$

$$R_m = \frac{L_m 2\pi f_s}{Q_s} \tag{5d}$$

$$R_o = \frac{1}{Q_p C_0 2\pi f_p} \tag{5e}$$

$$R_s = R_{\square} . \frac{L}{W} . \tag{5f}$$

The MBVD model of each resonator is optimized by minimizing a cost function, which measures the error between scattering (S) parameters and electrical specifications (filtering pattern). The specifications are defined by minimum or maximum values of the scattering parameters and are known for frequency intervals covering the entire domain of interest.

The cost function (C) is computed by summing weighted errors at each frequency defined in the frequency plan:

$$C = \sum_{i=1}^{N} (w_{21}(f_i).(S_{21}^{curr}(f_i) - S_{21}^{spec}(f_i)) - w_{11}(f_i).(S_{11}^{curr}(f_i) - S_{11}^{spec}(f_i)))/N, \tag{6}$$

where f_i are N frequencies defined in the frequency plan, S_{ij}^{curr} is the current S parameters (in decibels), S_{ij}^{spec} is the specified S parameters (in decibels), and w_{ij} is the error weights.

The error weight (w_{ij}) is set to zero when the scattering parameter fulfills the pattern, i.e., when the current scattering parameter is lower (resp. upper) than the maximum (resp. minimum) value specified in the pattern. In practice, different weights are used for computing errors on S_{21} and S_{11} parameters with opposite signs in passband and stopbands.

Variable parameters, N electrode surfaces (N being the number of resonators), and two resonant frequencies (one for loaded resonators and one for unloaded resonators) are constrained by min–max values. These parameters are optimized iteratively by estimating the cost function and the minimization direction by gradient computation [14] in the multivariable space. Such a local constrained optimization can be easily developed thanks to standard algorithms available in computing software (e.g., Matlab, with function fmincon).

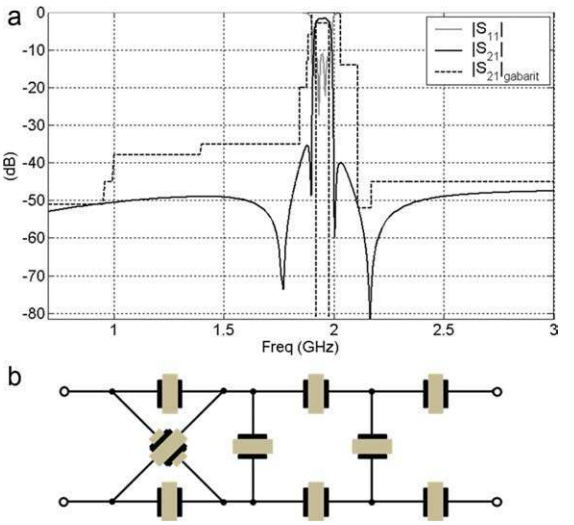

Figure 9 Simulated scattering parameters (a) and architecture (b) of the narrow-band bandpass filter. [Color figure can be viewed in the online issue, which is available at wileyonlinelibrary.com.]

The previous synthesis relies on MBVD models of BAW resonators, which do not take into account metallic losses or couplings due to interconnections and access ports. Because metallic lines used for connecting resonators have irregular geometries depending on the arrangement of resonators, models for such elements cannot be implemented in a synthesis tool. Nevertheless, a simulation is possible a posteriori with the layout of the filter to estimate additional losses or to check eventual couplings due to metallic lines.

The layout of the filter to be realized can be drawn with an EM software, e.g., momentum included in Agilent ADS. Using such an EM software, all electrostatic and EM phenomena are characterized considering the geometry and the physical characteristics of stacked layers.

The electrostatic part of MBVD resonators (R_s, R_o, and C_o) is directly taken into account in the distributed model (related particularly to the area of resonators). However, the motional part (R_m, C_m, and L_m) is modeled by lumped elements connected through internal ports.

C. Examples

1. Narrow-Band Bandpass Filter for UMTS Communications. The first example is a narrow-band bandpass filter designed for UMTS communications (Tx band). The fractional bandwidth is about 3%, which is consistent with typical electromechanical coupling coefficients of AlN (6–7%). The filter is implemented in SMR technology with differential input/output ports. For the application, a high selectivity and a high rejection are required. To attain such specifications, a mixed ladder–lattice configuration is selected as shown in Figure 9.

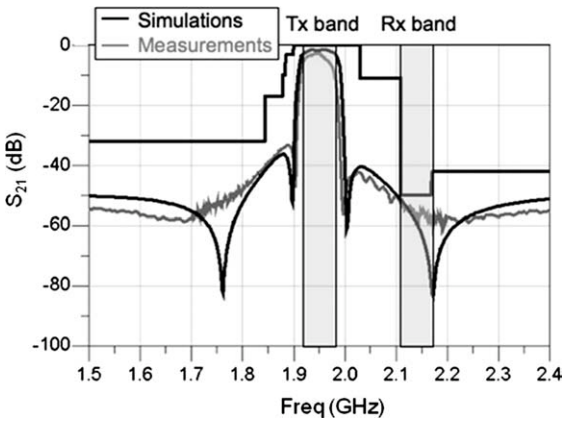

Figure 10 Measured scattering parameters of the narrow-band bandpass filter.

The filter has been fabricated and measured. The measurements presented in Figure 10 are in good agreement with simulated results, especially for the out-of-band attenuation. The passband of the fabricated filter is diminished because of a slight reduction of the resonant frequency for series resonators due to a poor trimming of the loading layer.

2. Wide-Band Bandpass Filter for Satellite Communications. The second example is a wide-band bandpass filter for space application. The fractional bandwidth is now 25%, which cannot be attained with an AlN BAW resonator. To achieve such a wide passband, $LiNbO_3$ BAW resonators are investigated. The $Y + 36^\circ$ crystallographic cut provides a thickness mechanical resonance with an electromechanical coupling that complies with the application (k_t^2 up to 37.5%). Figure 11 presents the response of a single lattice network optimized with respect to the specifications, demonstrating the potential of $LiNbO_3$ BAW resonators for wide-band filtering.

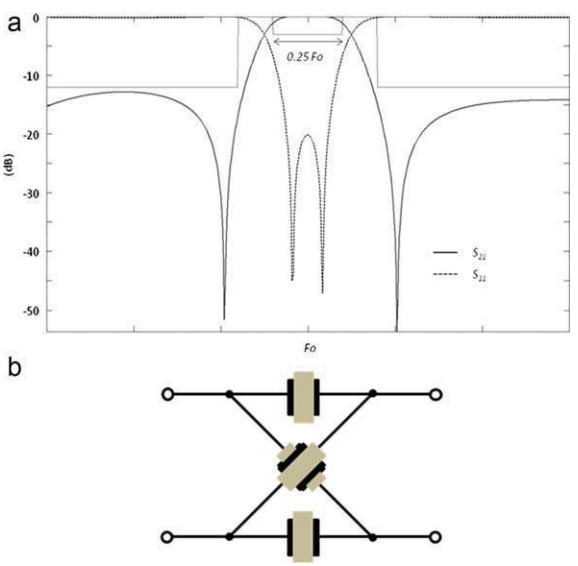

Figure 11 Simulated scattering parameters (a) and architecture (b) of the wide-band bandpass filter. [Color figure can be viewed in the online issue, which is available at wileyonlinelibrary.com.]

IV. CONCLUSION

A general approach is proposed for the design of BAW resonator filters. The procedure is based on a gradient-based optimization of MBVD resonator models. Such a model assumes a single (longitudinal or transverse) electromechanical resonance, and its lumped elements are directly related to the technological parameters. From this model, the surface of each resonator, the thickness of the piezoelectric layer, and the thickness of the loading layer can be optimized and a layout can be derived. A more precise characterization of the layout can be performed with an EM modeling of the circuit to consider additional losses and parasitic couplings that can occur with connecting lines.

The approach has been illustrated by the design of a mixed ladder–lattice filter with AlN BAW resonators providing a passband of 3% for UMTS applications. Measurements of the fabricated filter are in good accordance with the specifications, validating the model and the proposed approach.

Finally, the use of $LiNbO_3$ BAW resonators has been explored for enlarging the bandwidth of microwave filters up to 25% for space applications.

ACKNOWLEDGMENTS

This work has been conducted in the frame of two research projects: MOBILIS (FP6 IST European project) and FOVETTES (CNES, French Space Agency).

REFERENCES

1. R. Aigner, MEMS in RF-filter applications: Thin film bulk acoustic-wave technology, Digest of Technical Papers—International Conference on Solid State Sensors and Actuators and Microsystems, TRANSDUCERS '05, Seoul, Korea, Vol. 1, 2005, pp. 5–8.
2. R. Weigel, D.P. Morgan, J.M. Owens, A. Ballato, K.M. Lakin, K. Hashimoto, and C.C. Ruppel, Microwave acoustic materials, devices, and applications, IEEE Trans Microwave Theory Tech 50 (2002), 738–749.
3. R. Ruby, P. Bradley, D. Clark, D. Feld, T. Jamneala, and K. Wang, Acoustic FBAR for filters, duplexers and front end modules, IEEE MTT-S Int Microwave Symp Dig 2 (2004), 931–934.
4. K.M. Lakin, A review of thin-film resonator technology, IEEE Microwave Mag 4 (2003), 61–67.
5. S. Giraud, S. Bila, M. Chatras, D. Cros, and M. Aubourg, Bulk acoustic wave filters synthesis and optimization for multi-standard communication terminals, IEEE Trans Ultrason Ferroelectr Freq Control 57 (2010), 52–58.
6. D. Royer and E. Dieulesaint, Elastic waves in solids, Springer, Berlin, 2000; ISBN: 9783540659327.
7. Y. Fujiwara and N. Wakatsuki, $LiTaO_3$ and $LiNb0_3$ strip-type resonators, IEEE Trans Ultrason Ferroelectr Freq Control 34 (1987), 39–44.
8. Y. Osugi, T. Yoshino, K. Suzuki, and T. Hirai, Single crystal FBAR with $LiNbO_3$ and $LiTaO_3$ piezoelectric substance layers. IEEE MTT-S Int Microwave Symp Dig, 2004, pp. 873–876.

9. J. Fan, M. Chatras, and D. Cros, Synthesis method for BAW filters computation, Proceedings of the IEEE International Conference on Electronics, Circuits, and Systems, Nice, France, 2006, pp. 391–394.
10. J.D. Larson III, P.D. Bradley, S. Wartenberg, and R.C. Ruby, Modified Butterworth Van-Dyke circuit for FBAR resonators and automated measurement system, Proc IEEE Ultrasonic Symp 1 (2000), 863–868.
11. G.G. Fattinger, R. Aigner, and W. Nessler, Coupled bulk acoustic wave resonator filters: Key technology for single-to-balanced RF filters, IEEE MTT-S Int Microwave Symp Dig 2 (2004), 927–929.
12. K.M. Lakin, Bulk acoustic wave coupled resonator filters, Proceedings of the Annual IEEE International Frequency Control Symposium, New Orleans, Louisiana, United States, 2002, pp. 8–14.
13. A.A. Shirakawa, P. Jarry, J.-M. Pham, E. Kerhervé, F. Dumont, J.-B. David, and A. Cathelin, Ladder-lattice bulk acoustic wave filters: Concepts, design, and implementation, Int J RF Microwave Comput-Aided Eng 18 (2008), 476–484.
14. T.F. Coleman and Y. Li, An interior, trust region approach for nonlinear minimization subject to bounds, SIAM J Optim 6 (1996), 418–445.